



# Simulation studies of the combined effect of mass transport and impurities on step growth

James F. Lutsko<sup>a,\*</sup>, D. Maes<sup>b</sup>

<sup>a</sup> Center for Nonlinear Phenomena and Complex Systems, Code Postal 231, Université Libre de Bruxelles, Boulevard du Triomphe, 1050 Brussels, Belgium

<sup>b</sup> Structural Biology Brussels, Vrije Universiteit Brussel, Pleinlaan 2, 1050, Brussels, Belgium

## ARTICLE INFO

Communicated by J.J. De Yoreo

### Keywords:

A2. Growth from solutions  
A1. Computer simulation  
A1. Impurities  
A1. Mass transfer  
A1. Growth models  
A1. Diffusion

## ABSTRACT

A new kinetic Monte Carlo simulation approach for crystal growth from solution is presented. The simulations include an explicit representation of an extended volume of solution above the crystal face and realistically treats voids within the forming crystal, step overhangs and concentration gradients in the mother solution. The effect of impurities on step growth is investigated and it is shown that the results depend on a complex interplay between concentration gradients in solution driven by the consumption of material during step growth, the lifetime of impurities on the crystal surface and the geometry of the steps.

## 1. Introduction

The modern understanding of crystal growth is based on the fundamental insights developed in the first half of the twentieth century, resulting in the landmark 1951 paper of Burton, Frank and Cabrera [1]. This work was the starting point for many subsequent developments as notably discussed by one of the prominent contributors to this subject, Alexander Chernov, upon the occasion of the 50th anniversary of the original publication [2]. The basic elements are well known: in classical growth, steps originate either via 2D nucleation on the crystal surface or from defects such as dislocations, and then spread by the binding of crystal molecules at kink sites. The role of mass transport both in the form of surface diffusion and of diffusion from solution, when applicable, in controlling growth rates has been stressed in particular in the work of Chernov [2,3]. Despite the challenges arising from the presence of multiple length scales (molecules and kinks, step fronts and crystal layers) and the associated range of time scales, it is now possible to directly observe many aspects of the process of crystal growth. For example, in experiment biological macromolecules are often used as model systems because their large size enables molecular resolution of the surface features (e.g., using AFM [4–6] or via confocal microscopy [7–9]).

Whatever the context – be it geological processes, the manufacture of pharmaceuticals, or any other – crystals almost never form in a pure environment and the role of impurities in impeding or promoting crystal growth is an important practical issue. This was also recognized from very early on and was addressed in the well-known model of

Cabrera and Vermilyea (henceforth, CV) [10] which still forms the starting point of most discussion of impurity effects. In the CV model for the effect of impurities that impede step growth, when a (more or less) planar step front encounters impurities on the crystal surface, it is pinned at the points in contact with the impurities. At first, the remaining step front continues to grow but the pinned points lead to a curved interface which, due to the Gibbs–Thompson effect, results in a lower effective supersaturation at the step front. If the radius of curvature of the step front – which is just half the typical distance between impurities – is greater than the critical radius for 2D island nucleation, then the finger can grow in the same way as a super-critical island will grow, despite its curved interface. However, if the radius is smaller than the critical radius, then growth is not possible and the step becomes pinned. A survey of recent literature supporting, refining and challenging the CV model can be found in Ref. [11], but it remains the most common paradigm.

Computer simulations offer another way of investigating crystal growth having the advantage of molecular resolution and complete control of conditions. Molecular-scale simulations of crystal growth have a long history, going back at least fifty years to the classic work of Gilmer and Bennema [12]. In order to study much larger systems and longer times than would be possible with direct molecular-dynamics simulations, simplifications are often introduced such as the use of lattice-based, stochastic models like kinetic Monte Carlo (kMC). Indeed, one of the oldest and best known models used to study crystal growth

\* Corresponding author.

E-mail address: [jlutsko@ulb.ac.be](mailto:jlutsko@ulb.ac.be) (J.F. Lutsko).

is the lattice-based, kMC Solid-On-Solid (SOS) model in which only the crystal surface is directly simulated (see, e.g. Ref. [13]). Even more coarse-grained are models that only describe the evolution of the step front itself, e.g. the recent work of Weeks et al. [14]. In recent work using a classic SOS model, the CV model was tested in detail and was shown to be lacking a great deal of important physics [11]. In particular, it was shown that the Gibbs–Thompson effect is *not* the determinant of the step-pinning threshold, but rather the more basic criterion of whether or not step growth lowers the free energy of the overall system: the crystal and the reservoir of crystal molecules (e.g. the solution) taken together. This in turn implies that the step-pinning threshold depends on details like the size of impurities and whether or not they are incorporated into the crystal. It was also shown that the residency time of impurities on the crystal surface plays a critical role in whether or not they impede step growth: even very high concentrations of impurities on the crystal surface have little effect on step growth rates if they attach and detach very quickly, partly because they are not incorporated into the growing crystal and partly because kink sites are only blocked a short time if the impurities move quickly. The refined paradigm resulting from this work is that step blocking is analogous to a first-order phase transition and that whether or not the free energy of the system is lowered by the adding a crystal layer is the only factor determining whether or not the transition (i.e. adding a layer) will take place. The CV criterion plays the role of defining the spinodal: when the concentration of impurities is below the CV threshold, there is no barrier to the growth of fingers between the impurities (analogous to the process of spinodal decomposition) but when the concentration exceeds the CV threshold, the system's free energy is first increased by the growth of fingers and only decreases when they become large enough and so this process requires stochastic fluctuations quite analogous to the process of nucleation [15].

Another insight coming from simulation was the demonstration that step-bunches, or macrosteps, could grow even when the concentration of impurities was high enough to completely arrest the growth of elementary steps [16]. This is possible because newly formed step faces contain few impurities and so growth up the step face is possible. However, the limitations of the SOS model which include the absence of overhangs, of voids in the crystal and the assumption of uniform supersaturation mean that its use to model a complex systems such as macrosteps with impurities is questionable. For this reason, we introduced an extension of the SOS model which includes an explicit representation of the solution above the crystal and which overcomes the objection that the supersaturation at the crystal face is forced to be uniform [17]. This was used to confirm the SOS results concerning macrosteps and to study the effects of fluid flow on the growth of pure crystals [18]. However, since it was a hybrid model it retained some of the limitations of the SOS simulations: in particular, a lack of overhangs and voids and required a complicated and subtle treatment of the interface between the crystal and the solution.

In the present work, we describe a new lattice-based kMC model in which all SOS-type constraints are removed, thus giving the most realistic description of step growth possible in this class of simulations. This means that rather than treating dynamically only the molecules comprising the surface of the crystal, as in the SOS model, together with those in the fluid, as in our previous work, we include *all* molecules in the crystal as full participants in the dynamics. If implemented naively, this would involve a large increase in computational effort for little gain since it would mean trying to move molecules in the bulk of the crystal which – having no empty neighbor sites in which to move – are almost all immobile. We eliminate most of this increase by monitoring the state of each molecule and only attempting to move molecules which are not immobilized by their environment. We present this algorithm in the next Section. Following this, we discuss the results of simulations of step growth for pure systems and in the presence of impurities. In both cases, concentration gradients in the solution mean that the supersaturation at the crystal surface can differ substantially from that

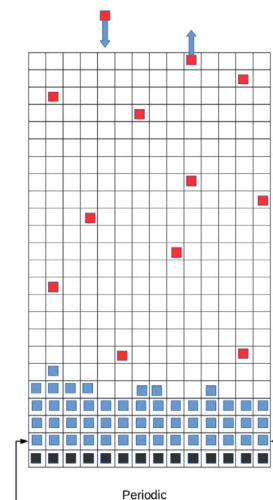


Fig. 1. A two-dimensional version of our simulation cell. The blue squares are molecules that are bound to the crystal. The black ones are also crystal molecules but they are “frozen” and do not move. The red squares are molecules in solution. Molecules in solution move by jumping to nearest neighbor sites and the upper boundary of the simulation cell is open with particles free to leave. Molecules randomly enter at the top boundary. The other (horizontal) boundaries are periodic. (For interpretation of the references to color in this figure legend, the reader is referred to the web version of this article.)

in the bulk solution. Furthermore, the effect of impurities is seen to be intimately tied to how strongly they bind to the crystal. The latter effect is found to be non-monotonic due to the two, opposing effects of lower impurity binding energy leads to fewer impurities being incorporated into the crystal while, at a fixed surface concentration, leading to a higher chance of impurities blocking kink sites. In the final section, we summarize the results and discuss future prospects for exploiting our novel simulation method.

## 2. Description of the algorithm

### 2.1. General overview

Our simulations take place on a cubic lattice with  $N_x \times N_y \times N_z$  sites and lattice spacing  $a$  with molecules that move from site to site on the lattice by means of jumps between Cartesian nearest neighbors (see Fig. 1). Periodic boundaries are applied in the lateral ( $x$ - and  $y$ -directions) while the  $z = 0$  plane is filled with fixed (immobile) crystal-species molecules to anchor the crystal. The top of the simulation cell (layer  $N_z$ ) is open and particles are free to jump out of the cell and, to compensate, molecules stochastically jump into the top-most layer with a frequency related to the super-saturation, as discussed below. All particles in the simulation cell, except those in the fixed bottom layer, are eligible to jump to any of its six nearest neighbor sites however, any such jump that is attempted fails if the destination site is already occupied. Hence, molecules with no empty neighbors are effectively immobile and we take advantage of this by only attempting moves for the population of mobile molecules. The fixed layer at the bottom is technically not necessary – the bottom could be treated the same as the top of the cell – but since almost all attempts to enter the simulation cell would be rejected, it is computationally more efficient to simply use the fixed layer boundary condition.

Physics enters via the interaction between molecules and via how they move. A molecule forms bonds with each of its nearest-neighbor molecules with the energy of the bonds depending on the species of the two molecules. In this work, we will take the crystal–crystal bond strength to be  $-\epsilon$ , independent of the direction of the bond. Since each bond is shared by the two participants, a molecule in the bulk has six

neighbors and a total energy of  $-3\epsilon$ . Our primary interest here is in systems with two species: a crystal-forming species A and an impurity species B and so we specify separately the crystal–crystal bond strength as  $\epsilon_{AA}$  and that between a crystal molecule and an impurity as  $\epsilon_{AB}$  and the impurity–impurity strength as  $\epsilon_{BB}$ . However, for brevity, we will simply write  $\epsilon_{AA} = \epsilon$  for the crystal–crystal bond.

The molecules move by making random jumps between Cartesian nearest neighbor sites following the standard kinetic Monte Carlo (kMC) algorithm. Since sites cannot be occupied by more than a single molecule, molecules that are surrounded by six occupied sites (e.g. most crystal molecules not on the surface) cannot move and are referred to as immobile: the rest are called mobile molecules. For reasons of efficiency, immobile molecules are not considered when deciding which molecule to move next so the only candidates are the  $N^{(k)}$  mobile molecules available after  $k$  kMC steps. Above the crystal is a virtual reservoir of molecules having a uniform density  $n_{SR}$  for each species  $S$  and, unlike in the simulation cell, molecules in the reservoir do not interact with one another (or with molecules in the simulation cell) so they are an ideal gas. Hence, besides the mobile molecules, there are also  $(n_{AR} + n_{BR})N_x N_y$  reservoir molecules that could jump in the  $-z$  direction and thus enter the simulation cell. Since each mobile molecule can potentially hop to one of six neighboring sites and each reservoir molecule can make only one relevant jump, the total number of possible moves for timestep  $k$  is  $6N^{(k)} + (n_{AR} + n_{BR})N_x N_y$ . A kMC step consists in randomly choosing one of these moves, testing whether it should be accepted and then, if so, executing it. Many moves will be rejected either because the target site is already occupied or for energetic reasons, as explained below. Whether or not accepted, the time is advanced by some amount  $\tau^{(k)}$ . In the following subsections, we discuss the details of the various elements.

## 2.2. Description of the dynamics

At every timestep, a molecule is chosen and an attempt is made to move it. To describe the dynamics succinctly, we collect the three Cartesian indices indicating the position of lattice site into “super indices” denoted by bold capital letters, e.g.  $\mathbf{I} = (I_x, I_y, I_z)$  and let  $n^{(k)}(\mathbf{I})$  be the number of molecules, or occupancy, at site  $\mathbf{I}$  at time-step  $k$ . We are interested in simulating multiple species so let  $n_S^{(k)}(\mathbf{I})$  be the number of molecules of species  $S$  at site  $\mathbf{I}$ . Clearly,  $n^{(k)}(\mathbf{I}) = n_A^{(k)}(\mathbf{I}) + n_B^{(k)}(\mathbf{I})$  and since each site can only be occupied by one molecule, all of these occupancies are either zero or one.

The dynamics follows the simple master equation

$$n_S^{(k+1)}(\mathbf{I}) = n_S^{(k)}(\mathbf{I}) + \sum_{\mathbf{J} \in \text{Neighbors of } \mathbf{I}} \left( P_{S\mathbf{J} \rightarrow \mathbf{I}}^{(k)} - P_{\mathbf{I} \rightarrow \mathbf{J}}^{(k)} \right) + \delta_{I_z, N_z} \left( P_{R \rightarrow S\mathbf{I}}^{(k)} - P_{S\mathbf{I} \rightarrow R}^{(k)} \right) \quad (1)$$

where the sum is over the Cartesian neighbors of point  $\mathbf{I}$  and  $P_{S\mathbf{J} \rightarrow \mathbf{I}}^{(k)}$  is the probability that a molecule of species  $S$  is at site  $\mathbf{J}$  at timestep  $k$  and that it hops to site  $\mathbf{I}$ . For sites with  $I_z < N_z$ , there will be six terms in the sum but in the top layer,  $I_z = N_z$ , there will only be five, with the third term on the right accounting for the interaction with the reservoir.

The probability of a move is the product of several factors,

$$P_{S\mathbf{J} \rightarrow \mathbf{I}}^{(k)} = n_S^{(k)}(\mathbf{J})(1 - n^{(k)}(\mathbf{I}))P_{\text{attempt } S\mathbf{J} \rightarrow \mathbf{I}}^{(k)}P_{\text{accept } S\mathbf{J} \rightarrow \mathbf{I}}^{(k)} \quad (2)$$

each of which we describe in turn. The first term is zero unless there is a molecule of species  $S$  at site  $\mathbf{J}$ , in which case it is one, while the second is one only if the site  $\mathbf{I}$  is unoccupied and is zero otherwise. This product simply means that there must be a molecule at site  $\mathbf{J}$  and none at site  $\mathbf{I}$  for the move to occur. The third factor is the “attempt probability”, i.e. the probability that out of all possible moves, this particular move, a jump from  $\mathbf{J}$  to  $\mathbf{I}$ , is chosen and actually attempted at timestep  $k$ , and the last factor is the probability that the jump is accepted. Special considerations apply to the sites at the top of the

simulation cell,  $I_z = N_z$ . These do not actually have a neighboring site at  $N_z + 1$  but in applying the algorithm we allow jumps in the  $+z$  direction in which case the molecule is removed from the simulation cell. For the reservoir this is modified to

$$P_{SR \rightarrow \mathbf{I}}^{(k)} = n_{SR}(1 - n^{(k)}(\mathbf{I}))P_{\text{attempt } SR \rightarrow \mathbf{I}}^{(k)}P_{\text{accept } SR \rightarrow \mathbf{I}}^{(k)} \quad (3)$$

$$P_{S\mathbf{I} \rightarrow R}^{(k)} = n_S^{(k)}(\mathbf{I})(1 - (n_{AR} + n_{BR}))P_{\text{attempt } S\mathbf{I} \rightarrow R}^{(k)}P_{\text{accept } S\mathbf{I} \rightarrow R}^{(k)}$$

The attempt probability is written as

$$P_{\text{attempt } S\mathbf{J} \rightarrow \mathbf{I}}^{(k)} = \nu_{S\mathbf{J} \rightarrow \mathbf{I}} \tau^{(k)} \quad (4)$$

where the attempt frequency,  $\nu_{S\mathbf{J} \rightarrow \mathbf{I}}$ , controls the speed of the particular physical process that the move produces. In our simulations, there are two attempt frequencies for each species. The first is  $\nu_{S0}$  which applies to jumps by molecules in the reservoir, in the solution in the simulation cell and for jumps between the solution and the crystal. The second is  $\nu_{S\text{Crystal}}$  which applies to moves by molecules which begin and end as part of the crystal: i.e. surface diffusion or diffusion within the bulk crystal (in the presence of vacancies). For each species, the jump frequency in the fluid directly determines the tracer diffusion constant of the molecules in solution, the jump frequency for crystal diffusion is directly related to the surface diffusion constant and the detachment frequency, determines e.g. the typical residency time of ad-atoms on the surface. For the other class of events – molecules moving from the reservoir to the site  $\mathbf{I}$  – the attempt probability is

$$P_{\text{attempt } SR \rightarrow \mathbf{I}}^{(k)} = \delta_{I_z, N_z} \nu_{S0} \tau^{(k)} \quad (5)$$

where the first factor assures that the site is in the topmost layer and  $\nu_{S0}$  is the attempt frequency for these moves. We note in passing that the time step  $\tau^{(k)}$  is not constant, as one might expect, but rather carries an index  $(k)$  since it will be seen below to depend on the number of particles in the simulation cell at any given moment and this changes during the simulation due to exchange with the reservoir.

The final contribution to the transition probability is the probability that the move is actually accepted,

$$P_{\text{accept } \mathbf{J} \rightarrow \mathbf{I}}^{(k)} = \min(1, e^{-\beta \Delta E(\mathbf{J} \rightarrow \mathbf{I})}) \quad (6)$$

where  $\Delta E(\mathbf{J} \rightarrow \mathbf{I})$  is the total change in energy of the system if the move is made and  $\beta = 1/k_B T$  is the inverse temperature. For reservoir jumps, the same expression is used with the understanding that molecules in the reservoir have no bond energy. This is the Metropolis criterion and ensures that the detailed balance relation

$$\frac{P_{\text{accept } \mathbf{J} \rightarrow \mathbf{I}}^{(k)}}{P_{\text{accept } \mathbf{I} \rightarrow \mathbf{J}}^{(k)}} = e^{-\beta \Delta E(\mathbf{J} \rightarrow \mathbf{I})} \quad (7)$$

holds which is necessary to produce an equilibrium state. Alternatives are possible: e.g. the acceptance probability could depend only on the energy needed to break any bonds that connect to the molecule at  $\mathbf{J}$  but without taking into consideration the bonds that will form after the move, but these will not be considered here.

## 2.3. The time-step

In general, one wants the timestep to be as large as possible so that the simulations are as efficient as possible: a small timestep means many attempted moves which result in nothing happening. The limiting factor on the timestep is that the sum of all probabilities must be less than or equal to one. Given the analysis above, it follows that the sum of the probabilities of all possible events is

$$\sum_{\mathbf{I}} \left( \sum_{\mathbf{J}} P_{\mathbf{I} \rightarrow \mathbf{J}}^{(k)} + \delta_{I_z, N_z} \left( P_{\mathbf{I} \rightarrow R}^{(k)} + P_{R \rightarrow \mathbf{I}}^{(k)} \right) \right) \leq 6N^{(k)} \max(\nu_{A0}, \nu_{A\text{Crystal}}, \nu_{B0}, \nu_{B\text{Crystal}}) \tau^{(k)} + (n_{AR} \nu_{A0} + n_{BR} \nu_{B0}) N_x N_y \tau^{(k)} \quad (8)$$

which is guaranteed to be less than or equal to one if we take

$$\tau^{(k)} \leq \frac{1}{6N^{(k)} \max(v_{A0}, v_{A\text{Crystal}}, v_{B0}, v_{B\text{Crystal}}) + (n_{AR}v_{A0} + n_{BR}v_{B0})N_xN_y} \quad (9)$$

and in practice one takes the upper limit. When multiple species are present, the obvious generalizations apply.

#### 2.4. Implementation

In our implementation of this algorithm, the system is first initialized with choices of simulation cell size, reservoir density, temperature and attempt frequencies. The molecules are separated into mobile and immobile molecules and those that form the crystal are identified and the total energy of the system  $E$  is calculated as is the initial timestep  $\tau^{(0)}$ . In the following use is made of the function  $\text{int}(x)$  which means the integer part of the real number  $x$  (e.g.,  $\text{int}(3.7) = 3$ ). It is also assumed that the nearest neighbor directions have been put into a list, e.g.  $(-\hat{x}, -\hat{y}, -\hat{z}, +\hat{x}, +\hat{y}, +\hat{z})$  so that they can be identified by integers from  $0 = -\hat{x}$  to  $5 = +\hat{z}$ . Then, the following loop is repeated where we use the function

1. Evaluate the timestep  $\tau^{(k)}$ .
2. Generate a pseudorandom number  $0 < r < 1$  and from it the random number  $R = r \times (6N^{(k)} + (n_{AR} + n_{BR})N_xN_y)$ .
3. Move
  - (a) If  $R < 6N^{(k)}$  then attempt to move mobile molecule  $n = \text{int}(R/6)$  in the direction corresponding to  $d = \text{int}(R - 6n)$ . Calculate the probability for this move,  $p_{\text{move}} = 0$  if the site is occupied, otherwise  $p_{\text{move}} = v_{\text{move}}\tau^{(k)}$  where  $v_{\text{move}}$  depends on the nature of the move and the species of the molecule.
  - (b) If  $6N^{(k)} \leq R$  choose a random site in layer  $z = N_z$  and calculate the attempt probability for a reservoir molecule to jump into this site as  $p_{\text{move}} = 0$  if the site is occupied and otherwise  $p_{\text{move}} = v_{S0}\tau^{(k)}$ . If  $R < n_{AR}N_xN_y$  the species is  $A$ , otherwise it is  $B$ .
4. Evaluate the energy,  $E'$ , of the new configuration that results if the move is accepted. Generate another pseudorandom number  $0 < s < 1$ 
  - (a) If  $s < p_{\text{move}} \min(1, \exp(-\beta(E' - E)))$  accept the move: update the energy to  $E$  and update the lists of mobile molecules and update the identification of molecules that are part of the crystal.
  - (b) Otherwise, reject the move and return to the initial state.
5. Update the time to  $t + \tau^{(k)}$ .

#### 2.5. Boundary conditions for step growth

If a step is parallel to the  $y$ -axis and growing in the  $x$ -direction, and its height at  $x = 0$  is  $z = H + 1$  then, until it reaches the end of the simulation cell, the height of the crystal at  $x = N_x - 1$  will be  $z = H$ . With periodic boundaries, when the step reaches the end of the simulation cell, molecules at position  $(x = N_x - 1, y, z = H + 1)$  will see neighbors at  $(x = N_x, y, z = H + 1) \rightarrow (x = 0, y, z = H + 1)$  and will therefore have the same number of bonds as any other surface molecule meaning that the surface layer will be complete and growth will stop, at least without a source for new steps such as 2D island nucleation. In order to allow step growth to continue when the step reaches the end of the cell, we use twist boundary conditions in which the periodic neighbor at  $(x = N_x, y, z) \rightarrow (x = 0, y, z + 1)$ . This allows step growth to continue indefinitely and does not affect the analysis given above except in one small detail. A molecule in solution

at the top layer of the simulation cell and at the  $x = N_x - 1$  edge, and so having coordinates  $(N_x - 1, y, N_z - 1)$  could hop to position  $x = N_x$ . With ordinary periodic boundaries, this would put it at  $(N_x, y, N_z - 1) \rightarrow (0, y, N_z - 1)$  but with twist boundaries, this instead gives  $(N_x, y, N_z - 1) \rightarrow (0, y, N_z)$  which means it leaves the simulation cell. In order to account for this additional loss of molecules, one must allow for the reverse process: namely, that a molecule can hop from the reservoir to any of the cells with coordinates  $(N_x - 1, y, N_z - 1)$  which means that in the formulas above, the quantities  $n_{SR}N_xN_y$  must be replaced by  $n_{SR}N_x(N_y + 1)$ .

#### 2.6. What is fluid and what is crystal?

In order to identify moves as detaching from the crystal or diffusing on the crystal, it is necessary to be able to classify molecules as forming part of the crystal or of being in the fluid. Each molecule carries a flag which is set to true if it is part of the crystal and false otherwise. We make this assignment via a clustering algorithm. First, all fixed molecules are labeled as crystal and all others are labeled as not-crystal. Then all neighbors of the existing crystal molecules are also labeled as crystal. This is repeated until no new crystal molecules are found. (Note that the actual implementation is much more efficient than this conceptual outline). During the simulation, every time a molecule attaches to the crystal (i.e. forms a bond with a molecule already tagged as part of the crystal) the attaching molecule is also tagged as part of the crystal. Similarly, whenever a molecule detaches from crystal it is tagged as being part of the fluid. In principle, when a molecule attaches to the crystal, it could also be in contact with another molecule which is in solution so that this second molecule should simultaneously become part of the crystal too. Similarly the reverse is possible when a molecule detaches. For this reason, the update of crystal molecules should extend to any neighbors of the attaching/detaching molecule (and of their neighbors and so forth). Such events are expected to be very rare except, e.g. in the roughening regime, and almost never occur in the conditions of the simulations reported here. Nevertheless, we repeat the clustering algorithm described above periodically to correct any misclassification.

#### 2.7. Impurities and directional bonds

Impurities are species other than the crystal-forming species. Each species is characterized by its own set of jump, detachment and diffusion attempt frequencies and a reservoir density as well as the inter-species and intra-species bond energies. Impurities can either impede or promote step growth depending on the crystal-impurity bond strength. An impurity that impedes growth might, e.g., have a crystal-impurity bond energy of zero. However, such an impurity will spend little time on the crystal surface and so would not in fact have much effect at all on step growth [11]. For this reason, we allow for impurities with a single directional bond: that is the impurity can form one bond with the crystal which has a different bond strength than bonds in any other direction: one might imagine an anisotropic molecule that has a single bonding site for the crystal species. In our implementation, we take the first attachment to the crystal to be the “binding site” and if the attachment has more than one possible binding direction (e.g. the case of attachment to a step face or a kink site) one of the available crystal neighbors is chosen randomly to be the binding neighbor. The strength of the directional bond then controls the residency time of the impurity on the crystal surface independently of the effect of the impurity on step growth.

#### 2.8. Limitations

The most important limitation of our simulation model is that we do not allow for the diffusion of multi-molecule complexes in the fluid as a whole. For example, if two molecules are neighbors in the fluid

then they will automatically bind to form a dimer. There is currently no provision for movement of the dimer as a whole: it can only change when one of its constituents detaches from the dimer. We hope to address this in future versions of the code.

A second limitation concerns impurities with directional bonds. The directional bonds will in general be quite strong – so that impurities have significant residency times on the crystal surface – but this causes a problem in the fluid since it becomes very likely that impurities will form dimers with a crystal-species molecule and hence (given the first limitation) become immobile. Furthermore, the likelihood of dissociation will be very low if the directional bond is strong. For this reason, we only allow directional binding to occur to the crystal itself and not to crystal-species molecules in solution.

### 3. Thermodynamic and kinetic properties of the simulations

Our main interest is the simulation of non-equilibrium phenomena such as step growth. However, in order to benchmark the algorithm and to make the connection to thermodynamics, we first consider the properties of equilibrium simulations. Our goal here is to translate the kMC algorithm into expressions for physical quantities such as the concentration of monomers in solution above the crystal and to thereby relate the parameters of the simulation to those quantities.

#### 3.1. Thermodynamics

The connection between the simulation algorithm and the underlying physics is obviously of paramount importance. In this Subsection we develop the connection on the basis of thermodynamic arguments. This complements a parallel analysis based on the kinetics of the molecules which has been given in detail elsewhere [18] and of which we briefly recall key elements in a subsequent subsection. For simplicity, we develop the thermodynamics for only a single species and drop the species index. The results are easily generalized to multiple species and are simply stated where appropriate.

##### 3.1.1. Simulation ensemble

To describe the thermodynamics of the system we must first define the ensemble. The results can be easily generalized as noted below. We view the reservoir as consisting of a (large) volume  $V_R$  with a number  $N_R^{(k)}$  of ideal gas molecules at any given timestep  $k$  so the total volume of the system is  $V_{\text{Total}} = V_{\text{Sim}} + V_R$  and the total number of molecules is  $N_{\text{Total}} = N_{\text{Sim}}^{(k)} + N_R^{(k)}$  and both quantities are constant. The simulation algorithm described above corresponds to taking the thermodynamic limit in which  $N_{\text{Total}}, V_{\text{Total}} \rightarrow \infty$  with  $N_{\text{Total}}/V_{\text{Total}} = n_{\text{Total}}$  held constant and in this limit the reservoir density is also  $n_R = n_{\text{Total}}$ . However, for conceptual clarity, we consider in this Section the thermodynamics for a large, but finite, system and only discuss the thermodynamic limit at certain points. The complete system therefore has fixed number of particles, temperature and volume and is thus canonical with free energy

$$F = U - TS = \sum_{\mathbf{I} \in \text{Sim}} E(\mathbf{I}) - TS \quad (10)$$

where the internal energy depends only on molecules in the simulation cell since the ideal gas molecules in the reservoir have no energy. The entropy is the sum of the entropies of the two subsystems, so

$$F = \sum_{\mathbf{I} \in \text{Sim}} E(\mathbf{I}) - TS_{\text{Sim}} - TS_R \quad (11)$$

$$= F_{\text{Sim}} + k_B T V_R (n_R \ln n_R \Lambda^3 - n_R)$$

where the last term on the right is the entropy of the ideal gas reservoir which depends on the thermal wavelength of the reservoir particles,  $\Lambda$ . Since particle number is constant, one has that  $n_R = (N_{\text{Total}} - N_{\text{Sim}})/V_R$  and the free energy is

$$\beta F = \beta F_{\text{Sim}} + (N_{\text{Total}} - N_{\text{Sim}}) \ln \frac{N_{\text{Total}} - N_{\text{Sim}}}{V_R} \Lambda^3 - (N_{\text{Total}} - N_{\text{Sim}}). \quad (12)$$

In the thermodynamic limit in which  $N_{\text{tot}}$  and  $V_R$  become large while  $N_{\text{Sim}}$  and  $n_R$  are held constant this can be expanded in  $N_{\text{Sim}}/N_{\text{Total}}$  to get

$$\beta F = \beta F_{\text{Sim}} - N_{\text{Sim}} \ln \left( \frac{N_{\text{Total}}}{V_R} \Lambda^3 \right) + N_{\text{Total}} \ln \left( \frac{N_{\text{Total}}}{V_R} \Lambda^3 \right) - N_{\text{Total}} + \mathcal{O} \left( \frac{N_{\text{Sim}}}{N_{\text{Total}}} \right) \quad (13)$$

which means that in the thermodynamic limit, the simulation subsystem is described by a grand-canonical ensemble with free energy

$$\Omega_{\text{Sim}} = F_{\text{Sim}} - \mu N_{\text{Sim}} \quad (14)$$

having chemical potential

$$\mu = k_B T \ln \left( \frac{N_{\text{Total}}}{V_R} \Lambda^3 \right). \quad (15)$$

One sees from this that the somewhat artificial ideal gas reservoir simply serves as a means of imposing a given chemical potential on the subsystem. When there are multiple species present, we denote the density of species  $S$  in the reservoir by  $n_{RS}$  and have that  $\mu_S = k_B T \ln (n_{RS} \Lambda^3)$ .

##### 3.1.2. Solution in equilibrium with the reservoir

The free energy of the system with no crystal present is

$$\Omega_{\text{Fluid}} = F_{\text{Fluid}} - \mu N_{\text{Fluid}}. \quad (16)$$

If one assumes the concentration in the solution is low, so that oligomers can be neglected, then the free energy of the solution is purely entropic and one has

$$\Omega_{\text{Fluid}} = k_B T N_{\text{Fluid}} \ln (n_{\text{Fluid}} \Lambda^3) - k_B T N_{\text{Fluid}} - \mu N_{\text{Fluid}} \quad (17)$$

which is minimized at constant volume by the equilibrium concentration  $n_{\text{Fluid}}^{(\text{eq})}$  that satisfies

$$\ln (n_{\text{Fluid}}^{(\text{eq})} \Lambda^3) = \beta \mu = \ln (n_R \Lambda^3) \quad (18)$$

so, as one might expect,  $n_{\text{Fluid}}^{(\text{eq})} = n_R$  which gives the usual ideal gas result

$$\Omega_{\text{Fluid}} = -k_B T N_{\text{Fluid}}. \quad (19)$$

Again, the generalization to multiple species is straightforward.

##### 3.1.3. Flat crystal in equilibrium with the solution

For a crystal to be in equilibrium with the fluid, the free energy of the system with a crystal with height  $H$  should be the same as a crystal of height  $H + 1$  (we measure  $H$  in units of the height of one lattice cell, so it is dimensionless). A perfect crystal has no entropy and an energy of  $-3\epsilon$  for each atom. We will also allow a number of vacancies  $N_V$  but will assume that the density of vacancies is small (and that the crystal volume is large) so that they may be treated as an ideal gas (i.e. we ignore vacancy dimers, surface effects, etc.). Then, each vacancy represents six broken bonds and so raises the energy by  $6\epsilon$  relative to the perfect crystal giving the crystal contribution to the free energy as

$$\Omega_{\text{Crystal}}(H) = (-3\epsilon - \mu) N_x N_y H + (6\epsilon + \mu) N_V + k_B T \left\{ N_V \ln \left( \frac{N_V}{N_x N_y} a^{-3} \Lambda^3 \right) - N_V \right\} \quad (20)$$

where the first term on the right is the energy of the perfect crystal, the second is the reduction of the energy due to vacancies and the last two (in brackets) are the entropy of the vacancies in the ideal gas limit (where  $a$  is the height of one lattice cell and  $\Lambda$  is the thermal wavelength). Of course, a crystal of height  $H$  reduces the volume accessible to the fluid, so again treating the fluid as an ideal gas, the total free energy will be

$$\beta \Omega_{\text{Sim}}(H) = \beta \Omega_{\text{Crystal}}(H) + N_{\text{Fluid}} \ln \left( \frac{N_{\text{Fluid}}}{N_x N_y (N_z - H)} \right)$$

$$-N_{\text{Fluid}} - \beta\mu N_{\text{Fluid}} + \beta F_{\text{Interface}} \quad (21)$$

where it is assumed that the interfacial contribution (i.e. the surface tension) is independent of  $H$  and where we have multiplied through by  $\beta$  and have dropped the irrelevant contribution of the thermal wavelength. Minimizing with respect to the number of vacancies gives

$$\frac{N_V}{N_x N_y H} = \exp(-6\beta\epsilon - \beta\mu) \quad (22)$$

and minimizing with respect to  $N_{\text{Fluid}}$  gives the expected result

$$\frac{N_{\text{Fluid}}}{N_x N_y (N_z - H)} = \exp(\beta\mu) \quad (23)$$

so

$$\beta\Omega_{\text{Sim}}(H) = \{(-3\beta\epsilon - \beta\mu)H - H \exp(-6\beta\epsilon - \beta\mu) - (N_z - H) \exp(\beta\mu)\} N_x N_y + \beta F_{\text{Interface}} \quad (24)$$

Thus,

$$\beta\Omega_{\text{Sim}}(H+1) - \beta\Omega_{\text{Sim}}(H) = \{(-3\beta\epsilon - \beta\mu) - \exp(-6\beta\epsilon - \beta\mu) + \exp(\beta\mu)\} N_x N_y \quad (25)$$

and this is zero for  $\beta\mu^{\text{(eq)}} = -3\beta\epsilon$  which is therefore the condition for crystal-fluid equilibrium, as one might expect. This therefore implies that the crystal-solution system will be in equilibrium when the solution concentration is

$$c_{\text{eq}} = \exp(\beta\mu_{\text{eq}}) = \exp(-3\beta\epsilon). \quad (26)$$

### 3.2. Kinetics

Since the kMC algorithm is stochastic, running it many times from the same starting configuration will yield different results. One can therefore discuss the occupancy of a cell averaged over many different runs,  $\langle n(\mathbf{I}) \rangle \equiv c^{(k)}(\mathbf{I})$ , which will be a real number between 0 and 1 and represents the concentration of the crystal-forming species. The detailed analysis of the results of applying this average to the fundamental dynamical equation, Eq. (1), is discussed in Appendix A and only the results will be discussed in this Section.

#### 3.2.1. Away from the crystal

In a fluid, with no crystal present, and at low concentrations so that the likelihood of any molecule having a neighbor can be neglected and  $\Delta E(\mathbf{I} \rightarrow \mathbf{J}) = 0$ , the average dynamics simplifies to

$$c^{(k+1)}(\mathbf{I}) = c^{(k)}(\mathbf{I}) + v_0 \tau^{(k)} \sum_{\mathbf{J} \in \text{Neighbors of } \mathbf{I}} \left( c_{\mathbf{J}}^{(k)}(\mathbf{J}) - c_{\mathbf{I}}^{(k)}(\mathbf{I}) \right) + v_0 \tau^{(k)} \delta_{I_z N_z} (n_{\mathcal{R}} - c^{(k)}(\mathbf{I})). \quad (27)$$

and away from the boundary, i.e. for  $I_z < N_z$ , the last term does not contribute so

$$\frac{c^{(k+1)}(\mathbf{I}) - c^{(k)}(\mathbf{I})}{\tau^{(k)}} = v_0 \sum_{\hat{\mathbf{e}}=\hat{x},\hat{y},\hat{z}} (c^{(k)}(\mathbf{I} + \hat{\mathbf{e}}) + c^{(k)}(\mathbf{I} - \hat{\mathbf{e}}) - 2c^{(k)}(\mathbf{I})) \quad (28)$$

which is recognized as the discrete form of the diffusion equation with diffusion constant  $D = v_0/a^2$ . In an equilibrium fluid, in which the concentrations are constant in both space and time  $c^{(k)}(\mathbf{I}) = n_{\text{Fluid}}$ , we see that

$$n_{\mathcal{R}} = n_{\text{Fluid}} \quad (29)$$

as was previously obtained from the thermodynamic description.

#### 3.2.2. Adatoms on the crystal

Consider a crystal with complete layers up to height  $z = H$  so that any molecules at  $z = H + 1$  are ad-atoms. In this short discussion, we allow for an arbitrary number of species and let the total number of ad-atoms of species  $S$  on the surface at timestep  $k$  be  $N_{\text{Sad}}^{(k)}$ . This changes

when a molecule in the fluid at level  $H + 2$  jumps down to level  $H + 1$ , thus joining the crystal, and when an existing ad-atom detaches and moves into the solution. Assuming that the concentration of molecules in solution is uniform in the x-y plane, and so depends only on the z-coordinate, we write  $c_S^{(k)}(\mathbf{I}) = c_S^{(k)}(I_z)$ . If  $-\epsilon_{AS}$  is the energy of a bond between a molecule of species  $S$  and the crystal surface, then the balance equation is

$$\frac{N_S^{(k+1)} - N_S^{(k)}}{\tau^{(k)}} = c_S^{(k)}(H+2) v_{S\text{Fluid}} \left( N_x N_y - \sum_{S'} N_{S'}^{(k)} \right) - N_S^{(k)} v_{S\text{Fluid}} e^{-\beta\epsilon_{AS}} \left( 1 - \sum_{S'} c_{S'}^{(k)}(H+2) \right) \quad (30)$$

where the terms in parenthesis are related to the probability that the end-point of the move is unoccupied. In equilibrium, the concentrations are independent of position and time,  $c_S^{(k)}(H+2) = c_S$ , giving the set of equations

$$N_S = \frac{c_S (N_x N_y - \sum_{S'} N_{S'})}{e^{-\beta\epsilon_{AS}} (1 - \sum_{S'} c_{S'})} \quad (31)$$

Solving this gives

$$N_S = \frac{c_S e^{\beta\epsilon_{AS}}}{(1 - \sum_{S'} c_{S'}) + c_S e^{\beta\epsilon_{AS}}} N_x N_y \quad (32)$$

or

$$N_S \simeq c_S e^{\beta\epsilon_{AS}} N_x N_y. \quad (33)$$

These relations allow us to use either the concentration of a species  $c_S$  or the fraction of surface occupied on average by this species, i.e. its surface coverage  $\sigma_S \equiv N_S/N_x N_y$ , using the relation

$$\sigma_S = \frac{c_S e^{\beta\epsilon_{AS}}}{(1 - \sum_{S'} c_{S'}) + c_S e^{\beta\epsilon_{AS}}} \approx c_S e^{\beta\epsilon_{AS}} \quad (34)$$

or, equivalently,

$$c_S = \frac{\sigma_S e^{-\beta\epsilon_{AS}}}{1 - \sigma_S} \frac{1}{1 + \sum_{S'} \frac{\sigma_{S'} e^{-\beta\epsilon_{AS'}}}{1 - \sigma_{S'}}} \approx \sigma_S e^{-\beta\epsilon_{AS}}. \quad (35)$$

## 4. Simulation results

Unless otherwise stated, all simulations were performed using a simulation cell of dimensions  $100 \times 40 \times 50$  at a temperature of  $k_B T = 0.25\epsilon$ . The simulations begin with three layers of perfect crystal with additional partial layers added for each step (e.g. one partial layer for single steps,  $n$  partial layers for step-trains of  $n$  steps). One of the goals of a simulation is to compute time-averages of various quantities as reported below. However, there is no point in updating the averages after every attempted move as the states of the system below and after a move are obviously highly coordinated. Thus, to control sampling the results we define a *cycle* to be  $\frac{1}{6} (6N^{(k)} + (n_{AR} + n_{BR})N_x N_y)$  elementary moves — in other words, approximately one attempted move per molecule and we typically update averages only after every 1000 cycles. The step velocity is determined from the time-average of the total number of molecules,  $M$  in the simulation volume. These are fitted to a straight line giving the slope,  $dM/dt$ , and the step velocity,  $\frac{1}{N_y} dM/dt$ , together with the corresponding standard errors. In the following, error bars show 2 standard errors of deviation in both directions. To give an idea of the simulations, Fig. 2 shows two snapshots of simulations of steps growing in the presence of impurities.

### 4.1. Control of thermodynamics

In the simulations, the concentration of crystal-forming species and of any impurities are controlled by the properties of the reservoir so it is necessary to establish how well one actually knows the physical

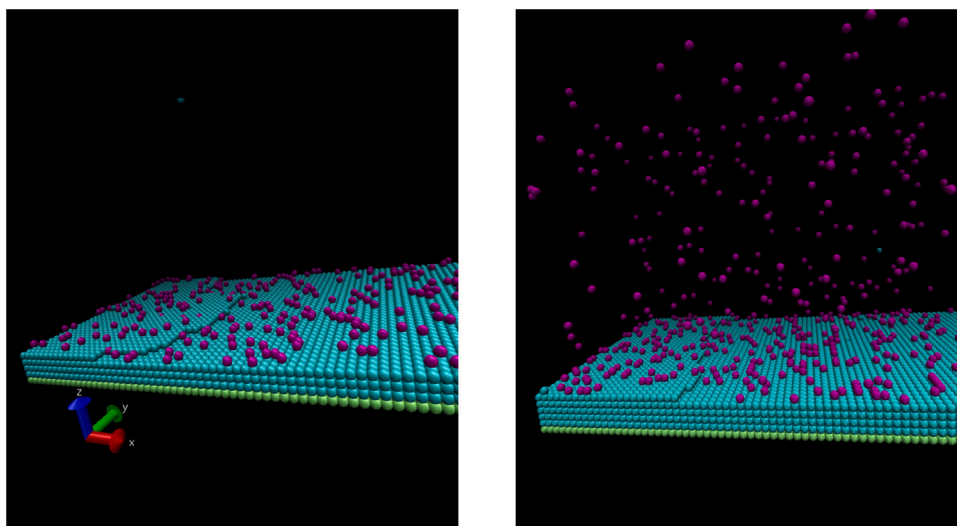


**Fig. 2.** Two snapshots from simulations of step growth. The left panel is for impurity binding strength  $\epsilon_{AB} = 4\epsilon_{AA}$ , the right panel is for  $\epsilon_{AB} = \epsilon_{AA}$  and both correspond to impurity coverage of 10% of the surface and reservoir supersaturation of  $\Delta\mu = 0.1\epsilon_{AA}$ . The lowest layer of the crystal is consists of static, fixed molecules shown in green, the crystal molecules are shown in blue–green and the impurities in purple. At this supersaturation the concentration of crystal molecules in solution is so low that only one appears in the image but the low impurity binding strength on the right requires a much higher concentration of impurities to maintain the surface coverage (from Eq. (35), approximately  $c_B = 1.1 \times 10^{-7}$  and 0.02, respectively). (For interpretation of the references to color in this figure legend, the reader is referred to the web version of this article.)

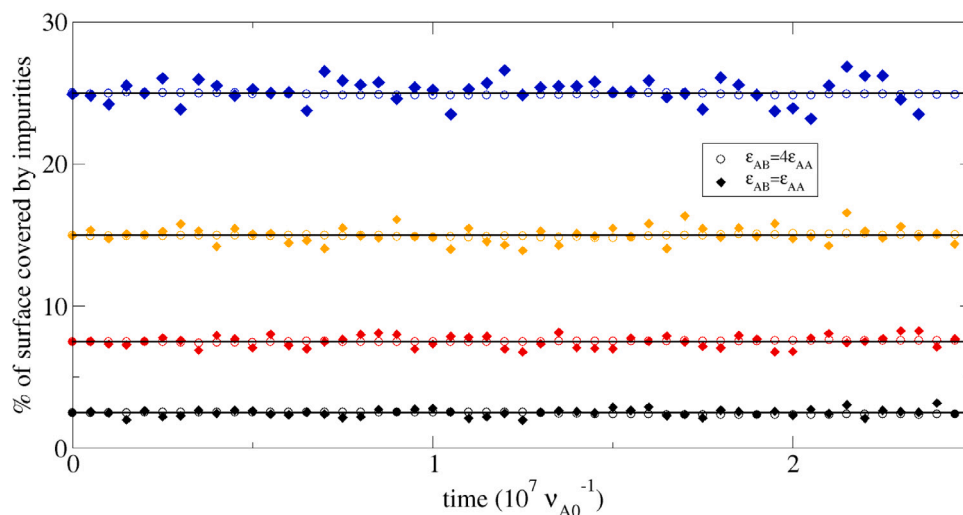


**Fig. 3.** Percent of a flat crystal surface covered by impurities as a function of time. The open circles correspond to strong impurity crystal bonds ( $\epsilon_{AB} = 4\epsilon_{AA}$ ) and the filled diamonds to weak bond ( $\epsilon_{AB} = \epsilon_{AA}$ ). The lines are the predicted coverage based on Eq. (32), which was the value used to initialize the simulations. The colors correspond to different imposed surface coverages: this imposed surface coverage and the impurity–crystal binding energy  $\epsilon_{AB}$  were inserted into Eq. (35) to determine the reservoir concentration used in each simulation. (For interpretation of the references to color in this figure legend, the reader is referred to the web version of this article.)

properties of the simulated fluid. Fig. 3 shows the observed coverage of a flat crystal surface by impurities as a function of time for strongly bound ( $\epsilon_f = 4\epsilon$ ) and weakly bound ( $\epsilon_f = \epsilon$ ) impurities agrees well with the coverage predicted by Eq. (32) even for coverages as large as 25% of the surface.

#### 4.2. Steps with no impurities

We begin with a single elementary step growing on an otherwise flat crystal surface. Fig. 4 shows the step velocity as a function of supersaturation of the reservoir. Note that because the concentration in the reservoir is constant, the system quickly reaches a steady state and so the step velocity is constant in time. In fact, as discussed below, the step velocity depends on the height of the fluid region between the crystal surface and the top of the cell and as the crystal adds layers, decreasing the size of this region, the velocity changes but

for sufficiently largest fluid regions, this change is very slow and can be ignored, as we do in the present discussion (for details, see the multiscale analysis given in Ref [18]). One usually thinks of step velocity as being proportional to supersaturation (or, equivalently at low supersaturation) to the excess concentration, but in the present case, one must ask “which supersaturation”? This is because as a step grows, it consumes material and therefore depletes the solution near the crystal surface. This constant depletion in turn gives rise to density gradients between the surface and the well-stirred region above the crystal (i.e. the reservoir), see Fig. 5. Fig. 4 demonstrates that there is indeed linear relation between the step velocity and the concentration at the crystal surface, even for very high supersaturation of the reservoir. Previous analysis has shown that the concentration should vary linearly over this region resulting in a relation between the step velocity,  $v$ , the concentration at the top of the simulation cell  $c(L_z) = c_R$  and the concentration at the crystal surface  $c(H)$ , where  $H$

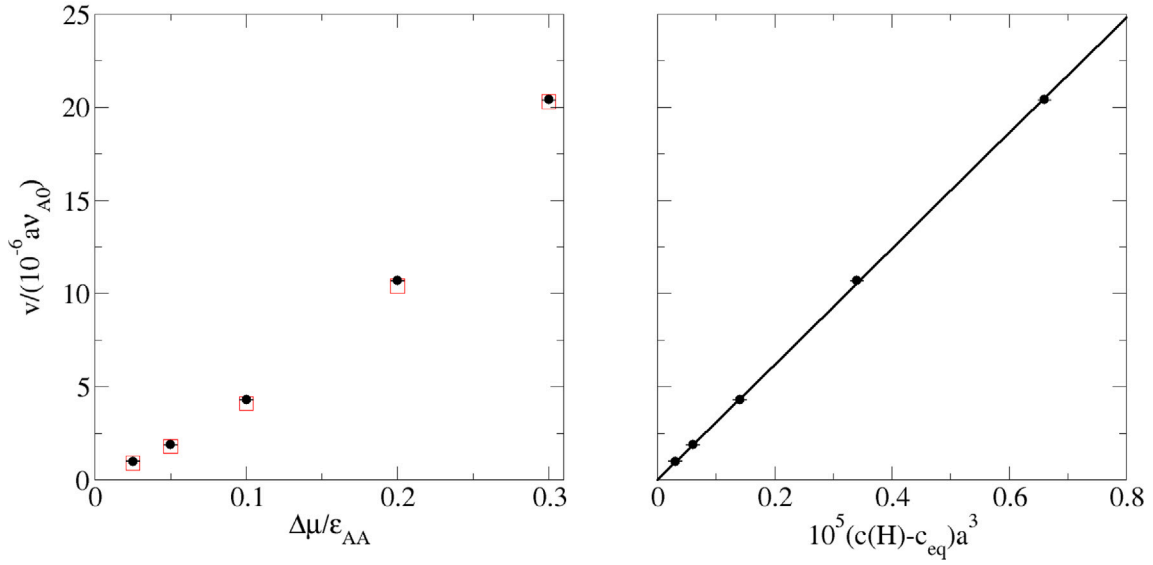


**Fig. 4.** Measured step velocities for  $k_B T = 0.25\epsilon_{AA}$  and a simulation cell of dimensions  $100 \times 40 \times 50$ . The left panel shows the velocities plotted as functions of the supersaturation of the reservoir (circles with error bars) as well as the prediction of Eq. (39), squares. The right panel shows the step velocities as functions of excess concentration measured at the crystal surface. The latter is highly linear as illustrated by the straight-line fit yielding a slope of approximately 3.1.

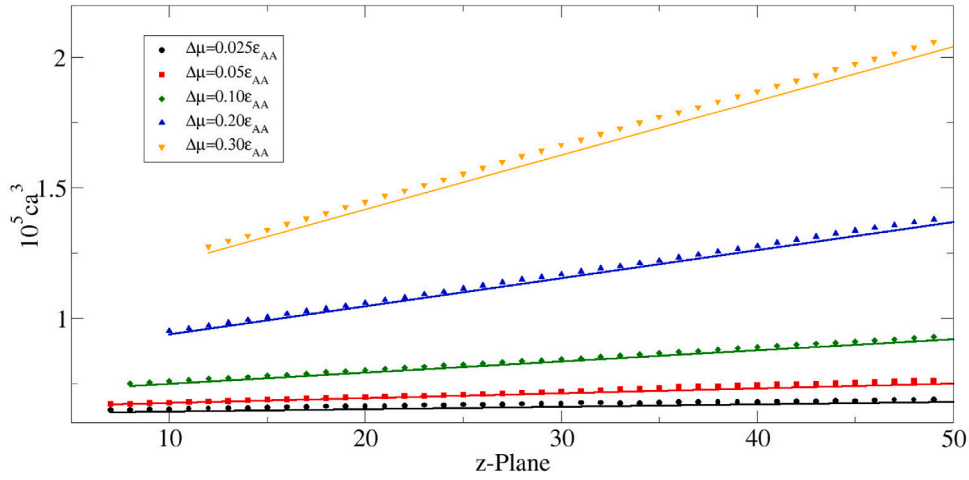


**Fig. 5.** Concentration gradients observed above a crystal surface with a single elementary step growing. The symbols show the simulation results and the lines are the predictions of Eq. (38). The expected linear variation of concentration from the reservoir (at  $z = 50a$ ) down to the crystal surface (near  $z = 10a$ , depending on the supersaturation) is observed. The difference between the predictions and the observed concentrations at the highest supersaturation are due to oligomers forming in the solution.

is the height of the crystal of

$$v(c(H)) = a^2 D (c_R - c(H)) \frac{L_x}{L_z - H} \quad (36)$$

where we recall that  $a$  is the distance between lattice sites and  $D = a^{-2} v_0$  is the tracer diffusion constant (see Eq. (28)). Note that the length of the simulation cell in the direction perpendicular to the step front enters this formula because all of the material at the crystal surface is, in principle, available for building the step.

Using the observed (see Fig. 4) variation of step velocity with surface concentration,  $v = \lambda(c(H) - c_{eq})$  with  $c_{eq} = \exp(3\beta\epsilon_{AA})$  and where the kinetic coefficient  $\lambda$  is taken from the fit to the data (see Fig. 4), gives

$$\lambda(c(H) - c_{eq}) = a^2 D (c_R - c(H)) \frac{L_x}{L_z - H} \quad (37)$$

allowing one to predict the surface concentration,

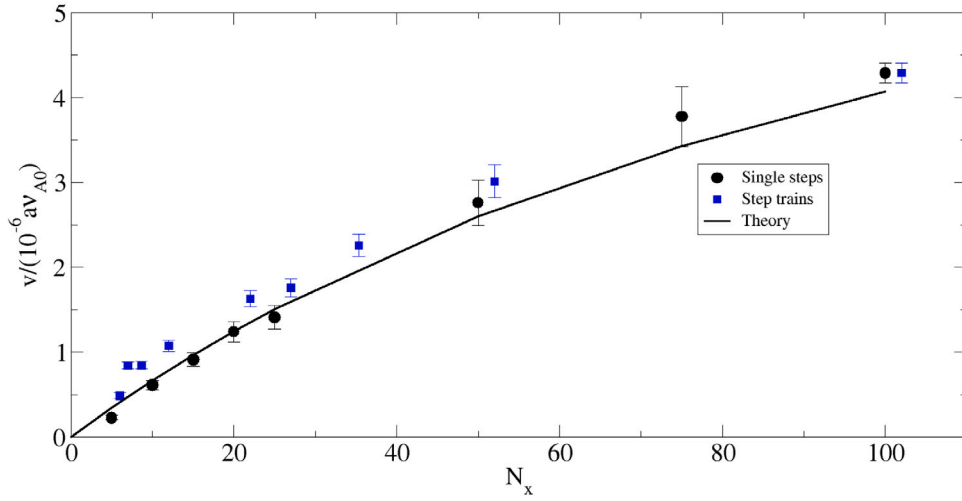
$$c(H) = c_R - \frac{\lambda}{\lambda + a^2 D \frac{L_x}{L_z - H}} (c_R - c_{eq}) \quad (38)$$

Fig. 5 shows that this prediction is quite accurate over the range of supersaturations considered here. The only significant deviation is at the largest supersaturation and is due to oligomers forming which are counted as contributing to the concentration but which do not participate in the mass transport due to the limitations of the algorithm as discussed in the previous Section. This results in an effective supersaturation at the crystal surface of about half that applied in the reservoir (e.g. for  $\Delta\mu/\epsilon = 0.025$  in the reservoir, it is 0.011 at the crystal surface and for 0.30 in the reservoir, one finds 0.18 at the surface).

Combining this expression for the concentration at the surface with the linear dependence of the step velocity on supersaturation at the surface gives the step velocity as a function of the reservoir concentration,

$$v(c_R) = \lambda \frac{a^2 D \frac{L_x}{L_z - H}}{a^2 D \frac{L_x}{L_z - H} + \lambda} (c_R - c_{eq}) \quad (39)$$

From this expression we learn several things:



**Fig. 6.** Measured step velocities for  $c_R a^3 = 0.1$ ,  $k_B T = 0.25 \epsilon_{AA}$  and a simulation cell of dimensions  $N_x \times 40 \times 50$  for different values of cell length,  $N_x$ . The full line is the prediction of Eq. (39) using the kinetic constant determined previously and the dashed line is the same formula fitting the kinetic constant,  $\lambda$ . The squares are the velocities obtained for step trains where the length of the simulation cell was fixed at  $N_x = 100$  and the number of steps,  $n_{\text{steps}}$  was varied from one to 25. The points are plotted at values of  $N_x$  corresponding to the average cell length available to each step, i.e.  $N_x = 100/n_{\text{steps}}$ . These points were then displaced slightly ( $N_x \rightarrow N_x + 2$ ) to avoid overlap with the single-step results.

1. The effect of the mass transport is to renormalize the kinetic coefficient so that  $v(c_R) = \bar{\lambda}(c_R - c_{\text{eq}})$  with the geometry-dependent kinetic coefficient

$$\bar{\lambda} = \lambda \frac{a^2 D \frac{L_x}{L_z - H_l}}{a^2 D \frac{L_x}{L_z - H_l} + \lambda} = \frac{\lambda}{1 + \frac{\lambda}{a^2 D} \frac{L_z - H_l}{L_x}} \quad (40)$$

- The strength of the renormalization is controlled by the product of two dimensionless parameters: the ratio of the rate of step growth and diffusion,  $\lambda/(a^2 D)$ , and the geometric factor consisting of ratio of the size of the boundary layer to the typical distance between steps,  $(L_z - H)/L_x$ .
2. In the regime of fast step growth and/or small distance between steps, compared to the boundary layer size,  $\frac{\lambda}{a^2 D} \frac{L_z - H_l}{L_x} \gg 1$ , the effective kinetic coefficient is  $\bar{\lambda} = a^2 D \frac{L_x}{L_z - H}$  and the rate of step growth is linear in step-separation and does not depend on the “bare” kinetic factor  $\lambda$  at all.
  3. In the regime of slow step growth and/or large distance between steps,  $\frac{\lambda}{a^2 D} \frac{L_z - H_l}{L_x} \ll 1$ , the difference in concentration between the reservoir and the step face is negligible and so the renormalized kinetic constant is nearly the same as the bare constant,  $\bar{\lambda} \simeq \lambda$ , corresponding to the situation assumed in SOS simulations.

Note that the third point says that when the steps are very widely spaced, the growth becomes “classic SOS”: conversely, when they are closer, their competition for material alters the growth rate. The meaning of “widely spaced” is that the distance between steps is large compared to the size of the boundary layer above the crystal.

The amount of material available to grow steps depends on the size of the crystal surface. In the case of multiple steps – i.e. step trains – this represents a competition between the steps for material. Eq. (39) predicts a non-trivial dependence of the step velocity on the length of the simulation cell and this is compared in Fig. 6 to the results of simulations. The analytic expression is seen to provide a good description of the dependence of step velocity on the length of the simulation cell. The figure furthermore shows that when holding the length of the surface constant but increasing the number of steps, the variation on step velocity is again mostly determined by the size of the terrace available to each step.

The fact that the step velocity depends on the length of the simulation cell in the direction of step growth is an important physical

effect that occur in our simulations with the explicit fluid that does not occur in SOS simulations. It is not a bug or artifact but, rather, a realistic effect that results from the fact that we never actually simulate individual steps: the periodic boundaries mean that we always simulate step-trains. In Ref. [18], it was shown that diffusion is fast compared to step growth so one can model the step growth quite well by averaging over the x-y plane. Thus the total amount of material available to incorporate into a step is that contained in the x-y plane above the crystal,  $c(H) N_x N_y$ . Since the amount of material needed for the step to grow one unit in the x-direction is proportional to  $N_y$ , this means the velocity is proportional to  $N_x$ .

#### 4.3. Steps with impurities

The impurities in our simulations are step blockers because they bind to the crystal surface (via a directional bond of strength  $\epsilon_{AB}$  but do not form bonds in other directions). The crystal-impurity bond strength determines the lifetime of an impurity on the surface, with the KMC dynamics giving the ad-impurity lifetime as  $\tau_I \approx v_0^{-1} e^{\beta \epsilon_{AB}}$ . Writing  $\epsilon_{AB} = \alpha \epsilon_{AA}$  and taking our standard condition,  $k_B T = 0.25 \epsilon_{AA}$ , this becomes  $\tau_I \approx v_0^{-1} e^{4\alpha} \approx v_0^{-1} 50^\alpha$ . In this study, there is no surface diffusion of impurities: they can only attach from the fluid and detach back into solution. In previous work using SOS models, we observed that impurities are only effective at blocking step growth when this lifetime is comparable to the time required for the step front to advance by one lattice constant. For typical step velocities of  $v \sim 10^{-6} av_0$  (see Fig. 6), this gives a threshold of  $\alpha \gtrsim 4$ . We also observed that the criterion for complete cessation of step growth, i.e. step pinning, is determined by thermodynamics: impurities raise the free energy of the crystal and when the impurity density is high enough, the total free energy is no longer reduced by adding crystal, so crystal growth stops. For impurities that occupy a single lattice site, as we study here, the resulting step-pinning threshold can be expressed, in the simplest approximation, as  $\sigma = \Delta\mu / (2\epsilon_{AA} + \Delta\mu)$  where  $\sigma$  is the (average) fraction of the surface sites occupied by impurities and  $\Delta\mu = k_B T \ln(c_R/c_{\text{eq}})$ .

The behavior with mass transport is considerably more nuanced than seen in the surface-only SOS simulations. One of the most important differences is due to the variation of the local density with step-velocity. As impurities are added to the surface, the step velocity decreases but this means that material is consumed from solution more slowly and so the local density at the surface of the crystal increases. This counteracts, to some extent, the decrease in step velocity caused

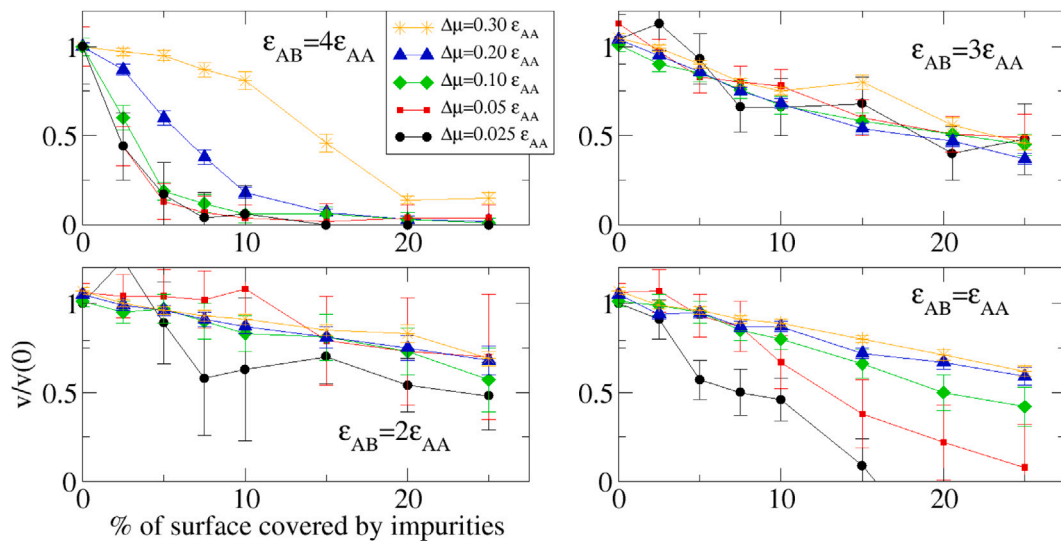


**Fig. 7.** Step velocity as a function of the density of impurities on the crystal surface (percent of surface covered by impurities) for various values of the impurity-crystal bond strength. The step velocities are normalized to their values with no impurities. This illustrates the dramatic effect that the lifetime of impurities on the surface has on the step-blocking properties of the impurities.

by the impurities. On the other hand, as the step velocity goes to zero and the steps become pinned, the concentration gradient disappears and the concentration at the crystal surface is the same as that of the reservoir so that the impurity concentration threshold above which steps are pinned is unaffected by the lowering of supersaturation at the surface. However, the expression for the threshold also assumes that all impurities are incorporated into the crystal, i.e. that they are completely pinned, and this is not the case thus leading to larger thresholds.

**Fig. 7** shows step velocities as a function of the surface coverage by impurities for various supersaturations (of the reservoir) and for various binding energies of the impurities to the crystal surface. At the strongest binding,  $\epsilon_{AB} = 4\epsilon_{AA}$ , one observes two distinct behavior. For  $\Delta\mu/\epsilon_{AA} = 0.025, 0.05$  and  $0.10$ , the step velocities scaled to their values with no impurities, collapse onto a single curve. Recalling the arguments from the previous Section, the balance between material transported by diffusion and that consumed in step growth should be unaffected, so that the effect of the impurities can be understood as changing the kinetic constant,  $\lambda$ . Indeed, assuming this is the case, we find that the generalization of Eq. (39) is

$$v(c_R, c_R^{(I)}) = \lambda(c_R^{(I)}) \frac{a^2 D \frac{L_x}{L_z - H_I}}{a^2 D \frac{L_x}{L_z - H_I} + \lambda(c_R^{(I)})} (c_R - c_{eq}) \quad (41)$$

so that the ratio  $v(c_R, c_R^{(I)})/v(c_R, 0)$  is independent of  $c_R$ , which is to say independent of supersaturation  $\Delta\mu = k_B T \ln c_R/c_{eq}$  as observed.

The data at higher supersaturations does not collapse onto the same curve as that at lower supersaturations. This is because, under these conditions, one observes nucleation of 2D islands for supersaturations of  $\Delta\mu \gtrsim 0.2\epsilon$ . For the pure systems discussed above, this was not a factor as the effective supersaturation at the crystal surface was about half of these values, and so did not exceed the 2D nucleation threshold. With impurities, this is no longer the case: as the impurities slow down the steps, the local supersaturation quickly rises and nucleation takes over. This accounts for the fact that at the highest supersaturation one observes little change in “step velocity” with impurity coverage until the latter becomes so high that the regions of free surface are disconnected and many nucleation events are necessary.

At lower impurity bond strengths, and so lower impurity residency time on the surface, the step-blocking effect first diminishes as expected. At  $\epsilon_{AB} = 3\epsilon_{AA}$ , the step velocity is only reduced a maximum

of 50% compared to the pure system, even at the highest coverage of the surface. At still lower impurity binding strength,  $\epsilon_{AB} = 2\epsilon_{AA}$ , the numerical noise in the results increases making it difficult to draw any conclusion except that the overall effect of impurities is somewhat diminished compared to stronger impurity binding. On the other hand, at the lowest binding strength,  $\epsilon_{AB} = \epsilon_{AA}$ , a dramatic change in behavior is evident: the strength of the impurity blocking is much stronger, with pinning observed for  $\Delta\mu = 0.025\epsilon_{AA}$  and possible for  $\Delta\mu = 0.05\epsilon_{AA}$  as well.

Another view of the data is given by **Fig. 8** which shows the step velocity as a function of impurity binding strength for moderate ( $\Delta\mu = 0.10\epsilon_{AA}$ ) and high ( $\Delta\mu = 0.30\epsilon_{AA}$ ) supersaturation. For lower coverage of the surface, the effect of the impurities is attenuated at low bond strength, as expected. However, at high coverage, there is a clear maximum in the step velocity and a lowering of the step velocity for the weakest impurity binding. **Fig. 9** shows the results for the lowest supersaturation,  $\Delta\mu = 0.025\epsilon_{AA}$  where the velocities systematically decrease below zero with increasing impurity coverage: in other words, adding impurities causes the crystal to dissolve. This is due to the impurities lowering the effective supersaturation of the crystal-forming species. In general, the rate at which molecules of a given species attach to a given spot on the crystal surface is  $v_0 c a^3$ , where  $c$  is the concentration of the species. However, if a site on the surface is occupied by an impurity, then it is blocked so that the rate of crystal molecules attaching to the surface is lowered. A short calculation, see **Appendix B** shows that in terms of molecules attaching to the crystal, the effective concentration at the crystal surface is  $c_{eff} = c(H)/(1 + \sigma)$  where  $\sigma$  is the proportion of the surface covered by impurities. This means that the effective supersaturation at the surface is  $\Delta\mu_{eff}(\sigma) = \Delta\mu_{eff}(\sigma = 0) - k_B T \ln(1 + \sigma)$  and that pinning will occur for  $\sigma = \exp(\beta\Delta\mu) - 1$ , with crystal dissolution occurring for larger coverages. For  $\Delta\mu = 0.025\epsilon_{AA}$ , this gives  $\sigma = 11\%$  and for  $\Delta\mu = 0.05\epsilon_{AA}$ ,  $\sigma = 22\%$  which are consistent with the data shown in the figures. Indeed, **Fig. 10** shows the predicted variation of the relative velocity as a function of surface coverage using Eq. (38) with  $c(H) \rightarrow c(H)/(1 + \sigma)$  and this is seen to be a good, semi-quantitative estimate of the observed step velocities.

One key question remains: why does this blocking effect only explain the data at weak impurity binding, since the behavior for strong binding is clearly different? The answer is ergodicity: the surface coverage and the relative time a given site is blocked by impurities are only

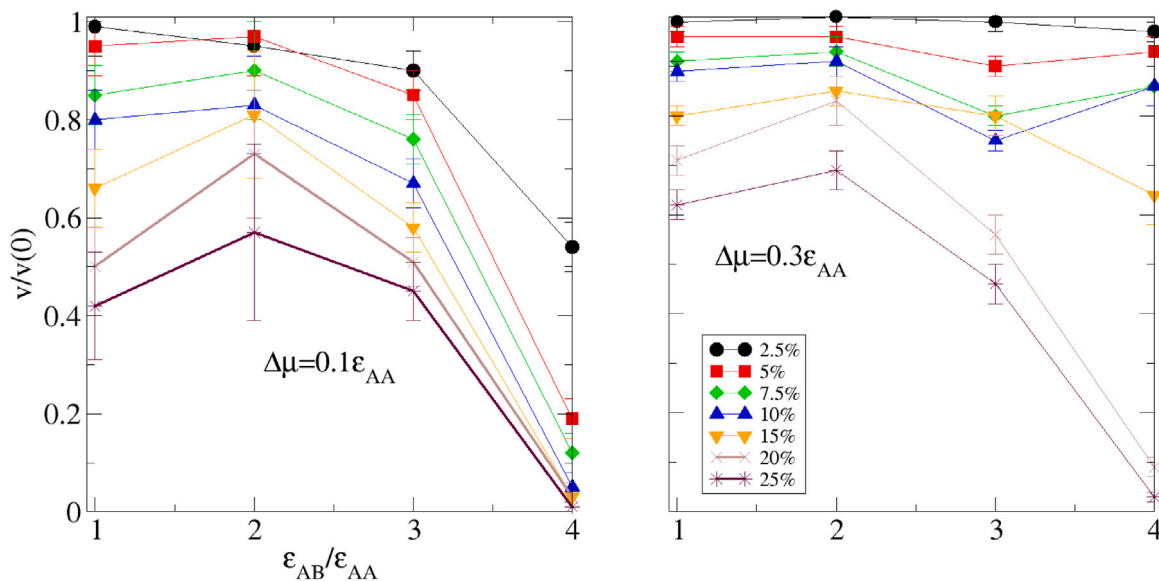


Fig. 8. Step velocity (normalized to a pure system) as a function of impurity binding strength for moderate supersaturation (left panel,  $\Delta\mu = 0.1\epsilon_{AA}$ ) and strong supersaturation (right panel,  $\Delta\mu = 0.3\epsilon_{AA}$ ). The curves are for different percentages of surface coverage by impurities. The lines connecting the points are just a guide for the eye.

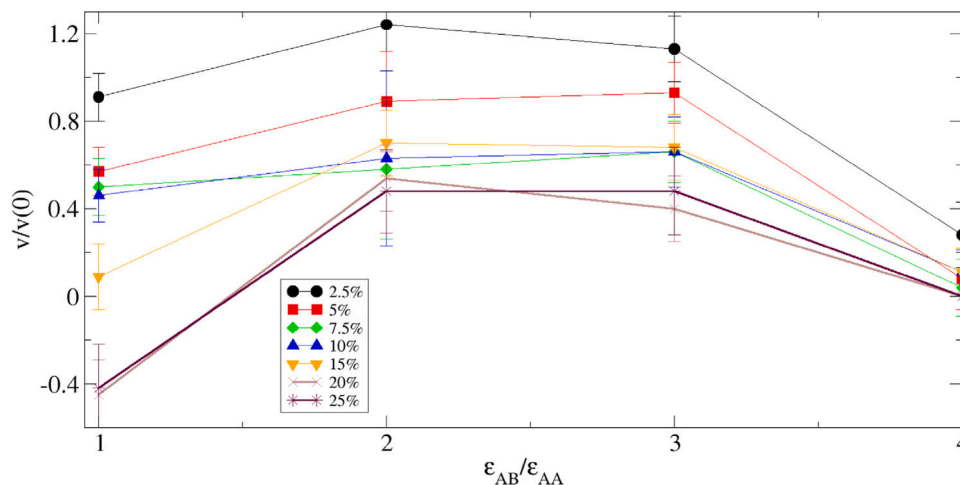


Fig. 9. The same as Fig. 8 for the case of low supersaturation,  $\Delta\mu = 0.025\epsilon_{AA}$ . Note the difference in scale compared to Fig. 8 which is due to the need to accommodate negative velocities.

comparable on time scales long compared to the impurity lifetime on the surface. When the impurities are strongly bound, their concentration in solution is very low and in the course of step growth, most kink sites will be filled with crystal molecules before an impurity can arrive and even those that do bind to the step are overcome by fluctuations before more impurities can arrive. So these arguments based on the blocking of individual sites are only valid in the limit that the impurity binding is weak and the timescale of exchange of impurities between the solution and the crystal surface is short compared to the timescale of step growth.

#### 4.4. Surface diffusion of impurities

The effect of impurities as step blockers decreases as they become less strongly bound to the interface due to the fact that they become more mobile. It is therefore not surprising that even for strongly bound impurities, surface diffusion has a similar effect. Fig. 11 shows the result of allowing surface diffusion of impurities to occur at the same rate as for crystal molecules at impurity binding energy  $\epsilon_{AB} = \epsilon_{AA}$ . For

all supersaturations, this level of surface mobility drastically reduces the ability of the impurities to block step growth.

### 5. Conclusions

We have described a fully unconstrained kinetic Monte Carlo algorithm for simulating crystal growth. It includes an explicit representation of the solution above the crystal and as such includes much more physics than surface-only models, such as the standard Solid-On-Solid simulation model. In particular, it gives a realistic description of mass transport in the solution and of its effect on crystal growth.

Simulating step growth in the presence of impurities revealed the effects of the interplay of mass transport and step growth. As previously noted [18], steady-state step growth leads to a linear concentration gradient in the quiescent boundary layer of fluid above the crystal. This in turn means that the step growth is driven by a supersaturation that is necessarily less than that in the bulk fluid. We developed simple expressions for the effective supersaturation at the crystal surface which accurately model the simulation results and that show the complex interplay between mass transport, step growth and geometry that make

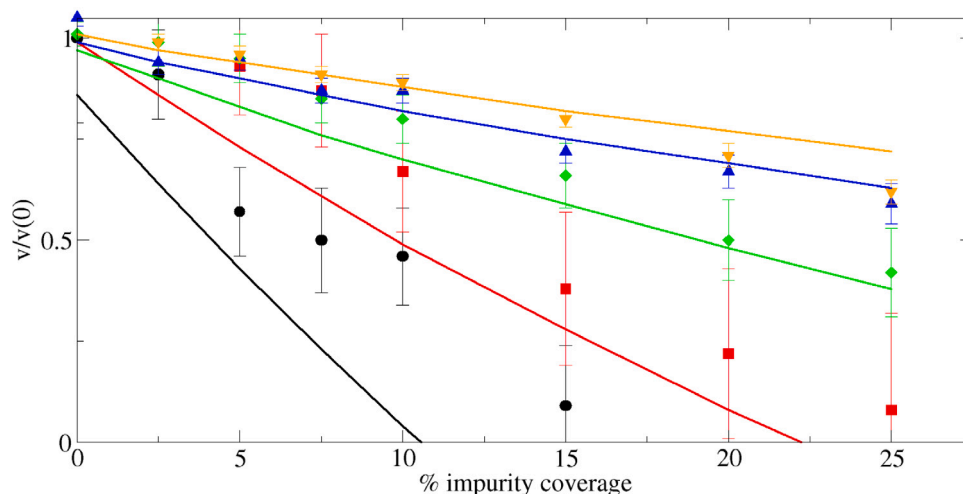


**Fig. 10.** Step velocity (normalized to a pure system) as a function of impurity coverage of the crystal surface for weak impurity binding,  $\epsilon_{AB} = \epsilon_{AA}$ : this is the same data and symbols as the fourth panel of Fig. 7. The lines are the theoretical prediction based on Eq. (38) with the surface concentration  $c(H)$  replaced by the reduced effective concentration,  $c(H)/(1 - \sigma)$  due to impurity blocking of surface sites.

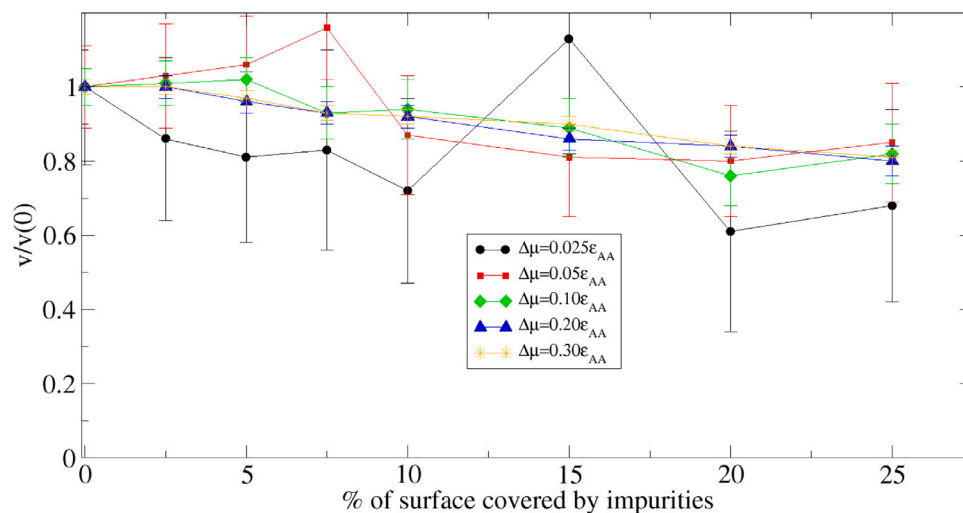


**Fig. 11.** Step velocity (normalized to a pure system) as a function of impurity coverage of the crystal surface for strong impurity binding,  $\epsilon_{AB} = 4\epsilon_{AA}$  and fast surface diffusion ( $v_{BCrystal} = v_{ACrystal} = v_{A0}$ ). This is the same data and symbols as the first panel of Fig. 7. Compared to that figure, one sees that the step-blocking power of the impurities is almost completely eliminated by the surface diffusion.

up the physical processes. One interesting consequence of this modeling is an explicit expression for the way step velocity depends on the (average) distance between steps in a step train.

The process of step growth becomes even more complex when impurities are introduced. Our impurities bind to the crystal surface but do not bind with any other crystal molecules (technically, the impurities are only allowed to bind to a single crystal molecule). Such impurities are expected to slow down step growth as their average surface concentration increases until at sufficiently high concentration they block step growth altogether. In fact, we find that this is only the case when the impurities bind very strongly to the crystal so that they are for all intents and purposes immobile. The threshold for such behavior is a very high bonding energy: even for a bond strength of four times the crystal–crystal bond strength, the effect of mobility already becomes apparent in a reduced sensitivity of the step velocity to impurity concentration. When the impurity bond strength is lowered to three times the crystal–crystal bond – the same as the binding energy of a crystal molecule in the bulk – the impurities cease to stop step growth and in fact the lowest step velocities at 25% impurity coverage were only about half of that of the pure system. Still lower impurity

bond strengths revealed a new surprise: the step velocity again drops but the reason is different than at high binding energies. In this regime, the impurity concentration is much higher (more than 50 times the crystal-forming species) in order to have the same surface coverage of impurities. The impurities bind and unbind from the surface rapidly and at such high concentrations block sites from the crystal molecules simply by occupying them. The effect, for which we again provided a simple model, is to lower still more the effective supersaturation at the crystal surface. In fact, for weak supersaturation in the bulk, the effect can manifest as the crystal dissolving due to increased impurity concentration.

There are still many questions that can be addressed using this type of extended simulation model. For example, in our analytic models we generally assume that the concentration can be treated as uniform in the x-y planes but, as stressed e.g. by Chernov [2], this is not the case near the crystal: just as step growth gives rise to concentration gradients in the direction perpendicular to the crystal, it also generates gradients at the crystal surface, in the direction of step growth. Our results somewhat mask this effect because we allow for relatively rapid surface diffusion and one might wonder in which domain this

assumption breaks down. Another question is the effect of fluid flow in the solution about the crystal on the phenomena discussed here. It is already known [18] that such flows have a dramatic effect on the growth of pure crystals and so it can be expected that they will generate additional complications in the presence of impurities. Finally, one of the original motivations for extending the simulation model beyond the surface-only SOS model was to realistically address the behavior of macrosteps. We hope to address these questions in future work.

### CRedit authorship contribution statement

**James F. Lutsko:** Conceptualization, Software, Investigation, Visualization, Writing – original draft, Writing – review & editing. **D. Maes:** Conceptualization, Investigation, Writing – original draft, Writing – review & editing.

### Declaration of competing interest

The authors declare that they have no known competing financial interests or personal relationships that could have appeared to influence the work reported in this paper.

### Data availability

Data will be made available on request.

### Acknowledgments

This work was supported by the European Space Agency, France under contract number ESA AO-2004-070. Computational resources have been provided by the Shared ICT Services Centre, Université Libre de Bruxelles and by the Shared ICT Services Centre funded by the Vrije Universiteit Brussel, the Flemish Supercomputer Center (VSC) and FWO.

### Appendix A. The averaged dynamics

Taking the average of the fundamental dynamical equation, Eq. (1), gives

$$c^{(k+1)}(\mathbf{I}) = c^{(k)}(\mathbf{I}) + \sum_{\mathbf{J} \in \text{Neighbors of } \mathbf{I}} \left( \langle P_{\mathbf{J} \rightarrow \mathbf{I}}^{(k)} \rangle - \langle P_{\mathbf{I} \rightarrow \mathbf{J}}^{(k)} \rangle \right) + \delta_{I_z N_z} \left( \langle P_{\mathbf{R} \rightarrow \mathbf{I}}^{(k)} \rangle - \langle P_{\mathbf{I} \rightarrow \mathbf{R}}^{(k)} \rangle \right) \quad (\text{A.1})$$

or

$$c^{(k+1)}(\mathbf{I}) = c^{(k)}(\mathbf{I}) + \tau^{(k)} \sum_{\mathbf{J} \in \text{Neighbors of } \mathbf{I}} \left( \langle n^{(k)}(\mathbf{J}) (1 - n^{(k)}(\mathbf{I})) v_{\mathbf{J} \rightarrow \mathbf{I}} \min(1, e^{-\beta \Delta E(\mathbf{J} \rightarrow \mathbf{I})}) \rangle - \langle n^{(k)}(\mathbf{I}) (1 - n^{(k)}(\mathbf{J})) v_{\mathbf{I} \rightarrow \mathbf{J}} \min(1, e^{-\beta \Delta E(\mathbf{I} \rightarrow \mathbf{J})}) \rangle \right) + \tau^{(k)} \delta_{I_z N_z} \left( n_{\mathbf{R}} v_{\mathbf{R}} \langle (1 - n^{(k)}(\mathbf{I})) \min(1, e^{-\beta \Delta E(\mathbf{R} \rightarrow \mathbf{I})}) \rangle - v_{\text{fluid}} \langle n^{(k)}(\mathbf{I}) \min(1, e^{-\beta \Delta E(\mathbf{I} \rightarrow \mathbf{R})}) \rangle \right) \quad (\text{A.2})$$

Consider now a crystal with (more or less) complete layers up to height  $z = H$  so that any molecules at  $z = H + 1$  are adatoms. Assuming the system is uniform in the x-y directions (parallel to the crystal face), the average occupancy will depend only on the z-coordinate which we can express as  $c_{\mathbf{I}}^{(k)} = c_{I_z}^{(k)}$ . Assuming also that both the concentration in the solution and the density of adatoms on the surface are low, the master equation for  $z = H + 1$  becomes

$$c^{(k+1)}(H+1) - c^{(k)}(H+1) = \tau^{(k)} \left( \langle n^{(k)}(\mathbf{I} + \hat{\mathbf{z}}) v_{\mathbf{I} + \hat{\mathbf{z}} \rightarrow \mathbf{I}} \min(1, e^{-\beta \Delta E(\mathbf{I} + \hat{\mathbf{z}} \rightarrow \mathbf{I})}) \rangle - \langle n^{(k)}(\mathbf{I}) (1 - n^{(k)}(\mathbf{I} + \hat{\mathbf{z}})) v_{\mathbf{I} \rightarrow \mathbf{I} + \hat{\mathbf{z}}} \min(1, e^{-\beta \Delta E(\mathbf{I} \rightarrow \mathbf{I} + \hat{\mathbf{z}})}) \rangle \right) \quad (\text{A.3})$$

where the first term on the right corresponds to a molecule in the fluid attaching to the crystal and the second to the detachment of an adatom. Writing  $\langle n^{(k)}(H+1) \rangle = n_{\text{adatom}}^{(k)}$  this becomes (neglecting correlations)

$$\frac{c_{\text{adatom}}^{(k+1)} - c_{\text{adatom}}^{(k)}}{\tau^{(k)}} = c_{H+2}^{(k)} v_{\text{fluid}} - c_{\text{adatom}}^{(k)} v_{\text{detach}} e^{-\beta \epsilon_{AA}} \quad (\text{A.4})$$

and for a system in equilibrium,

$$c_{\text{adatom}} = n_{\text{fluid}} \frac{v_{\text{fluid}}}{v_{\text{detach}}} e^{\beta \epsilon_{AA}} = \frac{c_{\text{fluid}}}{c_{\text{fluid}}^{\text{eq}}} \frac{e^{-2\beta \epsilon_{AA}}}{1 + (v_{\text{detach}}/v_{\text{fluid}}) e^{-3\beta \epsilon_{AA}}} \quad (\text{A.5})$$

### Appendix B. Waiting time

We ask here how long does it take, on average, for a site on the surface of the crystal to first be occupied by a crystal molecule? Let this waiting time be  $T$ , let the concentration of crystal molecules in the solution at the open site be  $c_A$  and let the concentration of impurities be  $c_B$ . If the site is unoccupied at time  $t = 0$  then in a short time interval  $\tau$  there are three possibilities: a crystal molecule arrives with probability  $p_A = c v_{A0} \tau$ , an impurity occupies the site with probability  $p_B = c_B v_{B0} \tau$  or nothing happens with probability  $(1 - p_A - p_B)$ . If an impurity lands, then it is necessary to wait some average time  $T_B^{(\text{detach})}$  for it to detach, after which the expected waiting time is again  $T$ . If nothing happens, then the expected waiting time starting at time  $t + \tau$  is also  $T$  so we expect that the waiting time is the sum of the probability of each of these three possibilities times the time associated with each one:

$$T = p_A \times \tau + p_B \times (\tau + T_B^{(\text{detach})} + T) + (1 - p_A - p_B) \times (\tau + T) \quad (\text{B.1})$$

The time for an impurity to detach can be developed the same way: it is the weighted sum of the possibility that it detaches in a time  $\tau$ , or it does not and then has to wait a time  $T_B^{(\text{detach})}$ ,

$$T_B^{(\text{detach})} = p_B^{(\text{detach})} \tau + (1 - p_B^{(\text{detach})}) (\tau + T_B^{(\text{detach})}) \quad (\text{B.2})$$

so  $T_B^{(\text{detach})} = \tau / p_B^{(\text{detach})}$  and using this in the expression for  $T$  and solving gives

$$T = \frac{1 + \left( \frac{p_B}{p_B^{(\text{detach})}} \right)}{p_A} \tau = \frac{1 + c_B e^{\beta \epsilon_{AB}}}{c_A} v_{A0}^{-1} = \frac{1 + \sigma}{c_A} v_{A0}^{-1} \quad (\text{B.3})$$

The effective concentration thus becomes  $c_A / (1 + \sigma)$  and the effective supersaturation  $\Delta \mu_{\text{eff}} = \Delta \mu - k_B T \ln(1 + \sigma)$ .

### References

- [1] W.K. Burton, N. Cabrera, F.C. Frank, The growth of crystals and the equilibrium structure of their surfaces, *Philos. Trans. R. Soc. Lond. Ser. A* 243 (1951) 299, proceedings of the Symposium - Progress in Crystal Growth.
- [2] A.A. Chernov, Notes on interface growth kinetics 50 years after Burton, Cabrera and Frank, *J. Cryst. Growth* 264 (2004) 499–518, proceedings of the Symposium - Progress in Crystal Growth.
- [3] A.A. Chernov, How does the flow within the boundary layer influence morphological stability of a vicinal face? *J. Cryst. Growth* 118 (1992) 333–347.
- [4] A. McPherson, A.J. Malkin, Yu.G. Kuznetsov, Atomic force microscopy in the study of macromolecular crystal growth, *Annu. Rev. Biophys. Biomol. Struct.* 29 (2000) 361–410.
- [5] S.-T. Yau, Dimitar N. Petsev, Bill R. Thomas, Peter G. Vekilov, Molecular-level thermodynamic and kinetic parameters for the self-assembly of apoferritin molecules into crystals, *J. Mol. Biol.* 303 (2000) 667–678.
- [6] Mike Sleutel, Celine Vanhee, Cécile Van de Weerd, Klaas Decanniere, Dominique Maes, Lode Wyns, Ronnie Willaert, The role of surface diffusion in the growth mechanism of triosephosphate isomerase crystals, *Cryst. Growth Des.* 8 (2008) 1173–1180.
- [7] Gen Sazaki, Alexander E.S. Van Driessche, Guoliang Dai, Masashi Okada, Takuro Matsui, Fermin Otalora, Katsuo Tsukamoto, Kazuo Nakajima, In situ observation of elementary growth processes of protein crystals by advanced optical microscopy, *Protein Pept. Lett.* 19 (2012) 743–760.
- [8] Mike Sleutel, Ronnie Willaert, Christopher Gillespie, Christine Evrard, Lode Wyns, Dominique Maes, Kinetics and thermodynamics of glucose isomerase crystallization, *Cryst. Growth Des.* 9 (2009) 497–504.

- [9] Mike Sleutel, Dominique Maes, Alexander E.S. Van Driessche, What can mesoscopic level in situ observations teach us about kinetics and thermodynamics of protein crystallization? *Adv. Chem. Phys.* 151 (2012) 223–276.
- [10] N. Cabrera, D.A. Vermilyea, Growth of crystals from solution, in: *Proceedings of the International Conference, Cooperstown, New York, 1958*, pp. 393–410.
- [11] James F. Lutsko, Nérido González-Segredo, Miguel A. Durán-Olivencia, Dominique Maes, Alexander E.S. Van Driessche, Mike Sleutel, Crystal growth cessation revisited: The physical basis of step pinning, *Cryst. Growth Des.* 14 (2014) 6129–6134.
- [12] G.H. Gilmer, P. Bennema, Simulation of crystal growth with surface diffusion, *J. Appl. Phys.* 43 (1972) 1347.
- [13] Yukio Saito, *Statistical Physics of Crystal Growth*, World Scientific, Singapore, 1998.
- [14] Madhav Ranganathan, John D. Weeks, Theory of impurity induced step pinning and recovery in crystal growth from solutions, *Phys. Rev. Lett.* 110 (2013) 055503.
- [15] Mike Sleutel, James F. Lutsko, Dominique Maes, Alexander E.S. Van Driessche, Mesoscopic impurities expose a nucleation-limited regime of crystal growth, *Phys. Rev. Lett.* 114 (2015) 245501.
- [16] James F. Lutsko, Alexander E.S. Van Driessche, Miguel A. Durán-Olivencia, Dominique Maes, Mike Sleutel, Step crowding effects dampen the stochasticity of crystal growth kinetics, *Phys. Rev. Lett.* 116 (2016) 15501.
- [17] Mike Sleutel, James Lutsko, Alexander E.S. Van Driessche, Mineral growth beyond the limits of impurity poisoning, *Cryst. Growth Des.* 18 (2018) 171.
- [18] Dominique Maes, James F. Lutsko, Molecular viewpoint on the crystal growth dynamics driven by solution flow, *Cryst. Growth Des.* 20 (2020) 2294.